Anti-CD3ε mAb improves thymic architecture and prevents autoimmune manifestations in a mouse model of Omenn syndrome: therapeutic implications

Veronica Marrella,[1,2] Pietro L. Poliani,[3] Elena Fontana,[3] Anna Casati,[4] Virginia Maina,[1,2] Barbara Cassani,[1,2] Francesca Ficara,[1,2] Manuela Cominelli,[3] Francesca Schena,[5] Marianna Paulis,[1,2] Elisabetta Traggiai,[5] Paolo Vezzoni,[1,2] Fabio Grassi,[4,6] and Anna Villa[1,7]

[1]Milan Unit, Istituto di Ricerca Genetica e Biomedica, Consiglio Nazionale delle Ricerche, Milan, Italy; [2]Humanitas Clinical and Research Center, Rozzano, Italy; [3]Department of Pathology, University of Brescia, Brescia, Italy; [4]Institute for Research in Biomedicine, Bellinzona, Switzerland; [5]Laboratory of Immunology and Rheumatic Disease, Istituto Giannina Gaslini, Genoa, Italy; [6]Dipartimento di Biologia e Genetica per le Scienze Mediche, Università di Milano, Milan, Italy; and [7]Telethon Institute for Gene Therapy, Hospital San Raffaele, Milan, Italy

Omenn syndrome (OS) is an atypical primary immunodeficiency characterized by severe autoimmunity because of activated T cells infiltrating target organs. The impaired recombinase activity in OS severely affects expression of the pre-T-cell receptor complex in immature thymocytes, which is crucial for an efficient development of the thymic epithelial component. Anti-CD3ε monoclonal antibody (mAb) treatment in RAG2$^{-/-}$ mice was previously shown to mimic pre-TCR signaling promoting thymic expansion. Here we show the effect of anti-CD3ε mAb administration in the *RAG2*^{R229Q} mouse model, which closely recapitulates human OS. These animals, in spite of the inability to induce the autoimmune regulator, displayed a significant amelioration in thymic epithelial compartment and an important reduction of peripheral T-cell activation and tissue infiltration. Furthermore, by injecting a high number of *RAG2*^{R229Q} progenitors into RAG2$^{-/-}$ animals previously conditioned with anti-CD3ε mAb, we detected autoimmune regulator expression together with the absence of peripheral immunopathology. These observations indicate that improving epithelial thymic function might ameliorate the detrimental behavior of the cell-autonomous RAG defect. Our data provide important therapeutic proof of concept for future clinical applications of anti-CD3ε mAb treatment in severe combined immunodeficiency forms characterized by poor thymus function and autoimmunity. (*Blood*. 2012;120(5):1005-1014)

Introduction

As opposed to the classic T$^-$B$^-$ severe combined immunodeficiencies (SCIDs), Omenn syndrome (OS) represents an atypical type of primary immunodeficiency (PID) associated with autoimmune manifestations because of activated oligoclonal T cells that infiltrate peripheral tissues and provoke generalized erythroderma, alopecia, lymphadenopathy, hepatosplenomegaly, and intractable diarrhea.[1] Patients have high levels of serum IgE despite the absence of circulating B cells. From the genetic point of view, most OS cases result from hypomorphic mutations in RAG genes[2,3] that decrease but do not completely abolish V(D)J recombination activity, allowing the generation of an oligoclonal autoreactive T-cell repertoire.[4-7] To date, allogeneic hematopoietic stem cell transplantation (HSCT) is the only beneficial therapeutic approach, although at high risk because of the myeloablative conditioning regimens necessary to eliminate autoreactive T lymphocytes and achieve successful engraftment.[8-10] We have recently generated and characterized a knock-in *Rag2*^{R229Q} mouse model, carrying a hypomorphic mutation in the *Rag2* gene (R229Q), initially identified in patients with OS or with leaky SCID.[10-12] The *RAG2*^{R229Q} mouse model closely recapitulates the human disease as mice display an expansion of oligoclonal and activated T cells which infiltrate target organs including skin, gut, liver, and lung,[13] and high levels of serum IgE, despite a severe arrest of B-cell development in the bone marrow.[14] This mouse model shows an arrest at the CD4$^-$CD8$^-$CD44$^-$CD25$^+$ double-negative 3 (DN3) stage of thymocyte differentiation, resulting in thymic atrophy and severe depletion of CD4$^+$CD8$^+$ double-positive (DP) and mature CD4$^+$ or CD8$^+$ single-positive (SP) cells. As previously observed in OS patients,[15,16] thymi from *RAG2*^{R229Q} mice are small, lack corticomedullary demarcation, and show a significant decrease in the expression of autoimmune regulator (AIRE), which induce the transcription of tissue-restricted antigens (TRAs) and plays a key role in the negative selection of autoreactive thymocytes.[17,18] This observation has raised the hypothesis that a defect in central tolerance might contribute to the immunopathogenesis of OS favoring the escape of self-reactive T cells to the periphery.[19,20] Here we show that *RAG2*^{R229Q} mice lack mature medullary thymic epithelial cells (mTECs^{high}) and display down-regulation in the mRNA expression for AIRE and TRAs. It has been shown that anti-CD3ε mAb injection into RAG2$^{-/-}$ mice, by mimicking TCRβ-selection of immature thymocytes, expands TECs as a result of thymocyte/epithelial cross-talk.[21-23] Administration of anti-CD3ε mAb to *RAG2*^{R229Q} newborns induces thymus expansion and differentiation of mTECs with a lack of generation of potentially pathogenic mature T cells. These events correlated with a lack of peripheral immunopathology, thereby suggesting that anti-CD3ε mAb induction of thymic development

Submitted January 25, 2012; accepted June 13, 2012. Prepublished online as *Blood* First Edition paper, June 21, 2012; DOI 10.1182/blood-2012-01-406827.

The online version of this article contains a data supplement.

The publication costs of this article were defrayed in part by page charge payment. Therefore, and solely to indicate this fact, this article is hereby marked "advertisement" in accordance with 18 USC section 1734.

might constitute a pretransplantation treatment in immunodeficient patients in which lymphopenia is associated with poor thymus development and autoimmunity.

Methods

Mice

RAG2$^{-/-}$ mice on C57/BL6 background were purchased from Taconic Laboratories. 129Sv/C57BL/6 knock-in *RAG2*^{R229Q} mice were previously generated by our group as described.[13] The animal colonies were housed in specific pathogen-free facility. All procedures were performed according to protocols approved by the Institutional Animal Care and Use Committee.

Anti-CD3ε mAb in vivo treatment

Anti-CD3ε mAb (clone 145-2C11)[24] was purchased from BD Biosciences. *RAG2*^{R229Q} adult mice (5 weeks old) received 2 intravenous doses (50 μg each) at a distance of 10 days. *RAG2*^{R229Q} newborn were treated with 2 intraperitoneal doses (25 μg each) at day 3 and at day 13 after birth, respectively. In parallel, PBS was administered to adult and newborn mutant mice as control in each experiment.

Generation of hypomorphic chimeric mice

Ten days after a single intravenous injection of 100 μg of anti-CD3ε mAb or PBS, 5-week-old RAG2$^{-/-}$ mice were sublethally irradiated (3 Gy, Cesium source) and transplanted with 10^6 fetal liver (FL) cells obtained from *RAG2*^{R229Q} embryos at day 13.5 postcoitum (indicated as FL^{R229Q}). Chimeras were followed for 3 months in a pathogen-free facility and then killed.

Lymphocyte analysis by FACS

Single-cell suspensions from thymi, spleens, and LNs were prepared by meshing tissues in PBS supplemented with 2% FBS and 5mM EDTA, and stained with the following specific fluorescent-conjugated Abs purchased from either BD Biosciences or eBioscience Inc: anti-CD4^{APC}, anti-CD8^{efluor450}, anti-CD44^{FITC}, anti-CD62L^{PE}, anti-CD69^{FITC} and anti-TCRβ^{PE}. To detect intracellular cytokine production, peripheral T lymphocytes were cultured for 5 hours in the presence of PMA (50 ng/mL; Sigma-Aldrich), ionomycin (1 μg/mL; Sigma-Aldrich), and monensin (1 μg/mL; Sigma-Aldrich), and then intracellular IFN-γ and TNF-α were stained according to the manufacturer's instructions (eBioscience). Samples were acquired on a FACSCanto II system (BD Biosciences) and analyzed with FlowJo software (Version 7.6.1; TreeStar).

Thymic epithelial cells preparation and analysis by FACS

Thymi from RAG2$^{+/+}$ and *RAG2*^{R229Q} mice were minced with scissors in PBS and the fragments were enzymatically digested in RPMI 1640 added with 1 mg/mL of Collagenase D (Roche) and 40 μg/mL DnaseI (Roche) for 30 minutes at 37°C. After the incubation, supernatant was collected and new digestion medium was added. All supernatants collected during several digestion passages were filtered on a 100-μm filter (BD Biosciences). The final suspension containing thymic epithelial cells (TECs) was stained with anti-CD45^{Pecy7}, anti-Ly51^{PE} (6C3 clone), and anti-MHCII$^{e\text{-}fluor450}$ (eBioscience). At least 1 000 000 total events was acquired in a FACSCANTO II and the analysis was performed with FlowJo software.

Histology

After sacrifice, tissue samples were formalin-fixed and paraffin-embedded or snap-frozen in isopentane precooled in liquid nitrogen. Paraffin sections (2 μm) were used for routine hematoxylin and eosin (H&E) staining and immunohistochemistry; whereas CD4 and CD8 immunostains were performed on 5-μm-thick acetone-fixed cryostat sections. Immunostains were revealed by the Real EnVision Rabbit HRP-labeled polymer system (DakoCytomation) or biotinylated rabbit anti–rat mouse preabsorbed (1:200; Vector Laboratories) followed by streptavidin–conjugated HRP (DAKO). Chromogen reaction was developed by DAB (DAKO) and nuclei counterstained by hematoxylin. The following reagents were used: rat anti–mouse CD4 (clone RM4-5; BD Biosciences); rat anti–mouse CD8 (clone 53-6.7; BD Biosciences); rabbit anti-cytokeratin 5 (CK5, clone AF 138; Covance); rat anti-cytokeratin 8 (CK8, clone TROMA-I; Developmental Studies Hybridoma Bank, University of Iowa); rabbit anti-AIRE (kindly provided by Prof P. Peterson, University of Tartu, Tartu, Estonia); biotinylated UEA-1 (Vector Laboratories). Digital imagines were acquired by Olympus DP70 camera mounted on an Olympus Bx60 microscope, using Cell^F Imaging software (Soft Imaging System GmbH).

Analysis of the ratio between medullary area and cortical area and tissue-infiltration score

Evaluation of the cortical-medullary maturation was performed by morphometric analysis using Cell^F Imaging software. The medullary area and cortical area (M/C) was calculated by measuring both medulla and cortical areas for each thymus and expressed in μm^2.[25] AIRE expression has been quantitatively scored as number of AIRE$^+$ cells/mm^2 evaluated on 5 different thymic section levels (~ 10 μm away from each other) using Scanscope CS and Imagescope software (Aperio). The degree of peripheral tissue inflammation was double blinded scored using the following semiquantitative criteria: 0 (none or scarce cell infiltrates); 1 (low to moderate); 2 (moderate to high); 3 (very high). The specific CD4 and CD8 infiltration index was obtained by semiquantitative analysis counting the number of positive cells for each individual marker in 5 different high-power field (HPF) according to the following scheme: 0-5 positive cells (negative/low); 5-20 positive cells (moderate); > 20 positive cells (moderate/high).

RNA extraction and real-time PCR

Total RNA from whole RAG2$^{+/+}$ and *RAG2*^{R229Q} thymi were extracted with TRIzol reagent following the suggested protocol (Invitrogen) and then 1 μg of RNA was reverse transcribed using the High Capacity cDNA Archive Kit (Applied Biosystems) according to the manufacturer's instructions. AIRE, Insulin2, CytP450, FABP, and GAD67 expression was quantified by RT-PCR from 50 ng of cDNA in the presence of the TaqMan Universal PCR master mix (Applied Biosystems), 200nM gene-specific TaqMan probe (Universal Probes from Roche Applied Science), and 800nM of relative primer pairs, using the DNA Engine Opticon 2 System (MJ Research) with the following thermal conditions: 95°C for 10 minutes, 40 cycles of 95°C for 15 seconds, and 60°C for 60 seconds. The primers and probes used are the following: AIRE, GGTTCCTCCCCTTCCATCGGCACACTCATCCTCGTTCT probe 45; Insulin2, TGAAGTGGAGGACCCACAAAGTGCCAAGGTCTGAAGGTC probe 32; CytP450, GACTGACTCCCACAACTCTGCGAACGCCATCTGTACCACTG probe 19; FABP, ACGGAACGGAGCTCACTGTTACCAGAAACCTCTCGGACA probe 17; GAD67 AACCAGATGTGTGCAGGCTGTCCCCGGTGCATAGGAG probe 52; Cyclophillin TTCAAGCTGAAGCACTACGGATTGGTGTCTTTGCCTGCA probe 20. Each sample was analyzed in duplicates, and the relative expression of target genes were defined by calculating the D cycle threshold, with respect to the housekeeping gene (Cyclophillin).

ELISA

Levels of IgG isotypes, IgA, and IgM were measured in sera by the multiplex assay kit (Beadlyte Mouse Immunoglobulin Isotyping kit; Millipore) according to the manufacturer's instructions and run using a Bio-Plex reader (BioRad Laboratories). Levels of IgE were determined by ELISA assay (BD Biosciences).

Statistical analysis

Groups were analyzed with Prism software (GraphPad) using a 2-tailed Mann-Whitney unpaired test. Data are presented as mean ± SD. *P* values of < .05 were considered significant.

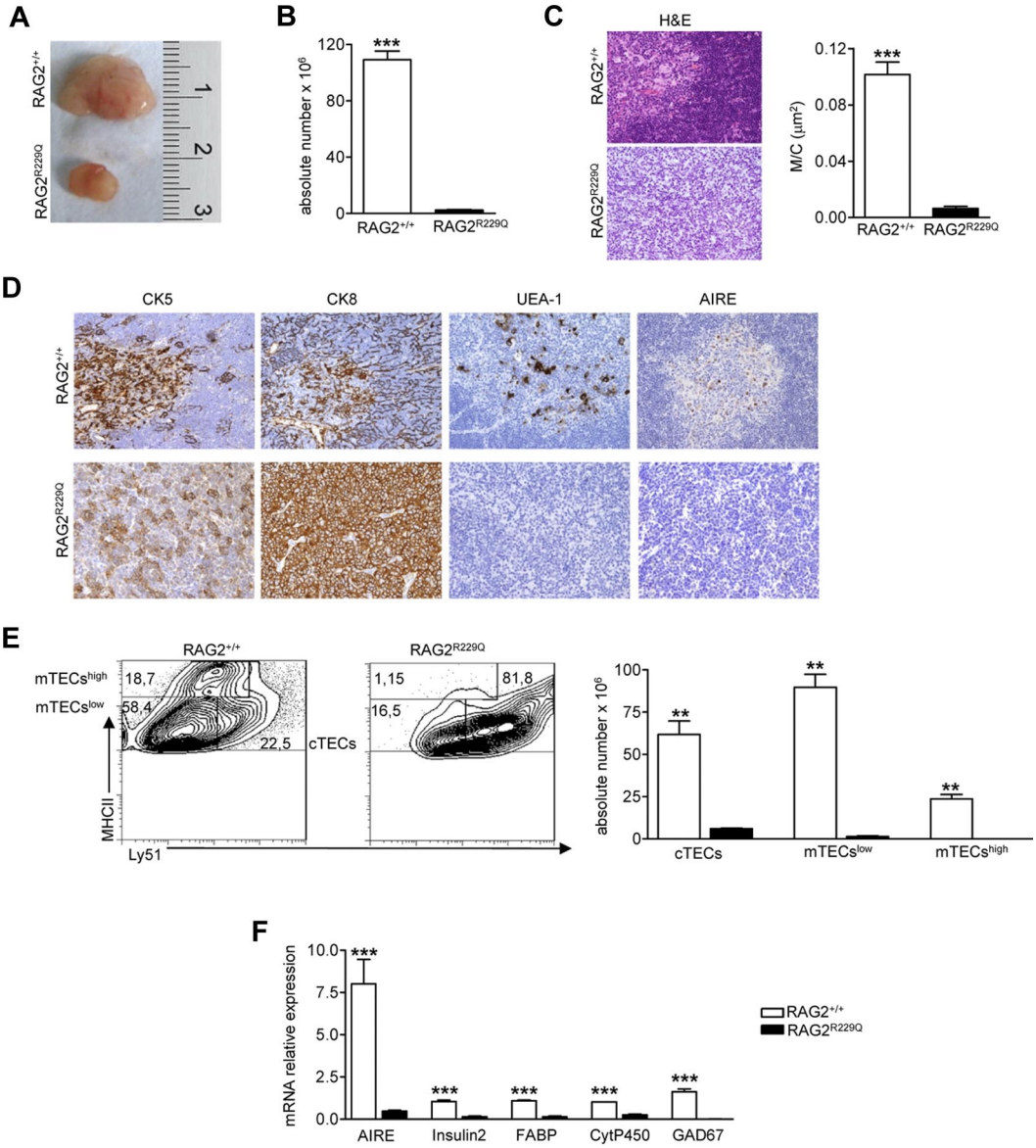

Figure 1. Thymic epithelial defect in *RAG2*^{R229Q} mice. (A) Macroscopic aspect of representative 5-week-old RAG2$^{+/+}$ and *RAG2*^{R229Q} thymus. (B) Thymic cellularity in RAG2$^{+/+}$ (n = 22) and *RAG2*^{R229Q} (n = 33) mice; ***$P < .0001$. (C) Representative H&E staining of thymus from a 5-week-old *RAG2*$^{+/+}$ and *RAG2*^{R229Q} mouse (original magnification, ×20) and graphic representation of the M/C in the indicated mice (n = 8); ***$P < .0001$. (D) CK5, CK8, UEA-1, and AIRE immunohistochemistry of 5-week-old RAG2$^{+/+}$ and *RAG2*^{R229Q} thymus (original magnification, ×20). (E left) FACS analysis of thymic stromal compartment: CD45^{-} fraction, obtained after enzymatic digestion was stained with MHCII and Ly51 Abs to identify the 3 different epithelial subsets. Numbers represent the percentage within the indicated regions. (Right) Absolute number of the different epithelial subpopulations obtained after enzymatic digestion of *RAG2*$^{+/+}$ and *RAG2*^{R229Q} thymi (n = 5); **$P = .0025$. (F) Real-time analysis of AIRE and indicated TRA transcripts on RNA extracted from total thymus of RAG2$^{+/+}$ (n = 4) and *RAG2*^{R229Q} mice (n = 4). Quantitative RT-PCR was run in triplicate (results are representative of 3 independent experiments); ***$P = .0007$.

Results

Impaired thymic architecture in *RAG2*^{R229Q} mice

Thymocyte/epithelium crosstalk crucially shapes thymus development and morphology. The correct maturation of thymic stromal component is instrumental in mediating the differentiation of a self-tolerant and self-MHC–restricted T-cell repertoire.[26] *RAG2*^{R229Q} thymi from 5-week-old mice showed a dramatic reduction in size (Figure 1A) and severe cell depletion (Figure 1B). H&E staining showed a compromised thymic architecture in *RAG2*^{R229Q} mice, further confirmed by a dramatic reduction of the M/C, which is an index of correct development of the organ (Figure 1C). In a normal thymus, differential expression of CK8 and CK5 distinguishes cortical TECs (cTECs), which are mainly CK8^{+}CK5^{-}, from mTECs showing prevalent CK5 expression.[27] In *RAG2*^{R229Q} thymi, the normal corticomedullary differentiation depicted by CK5 immunostaining was absent and CK8 distribution was altered because the framework of epithelial cells normally depicted by this marker was completely lacking. Moreover, the *RAG2*^{R229Q} thymi showed a severe depletion of *Ulex europeus* agglutinin-1 (UEA-1) positive mTECs, which were distributed within the thymic medulla in normal thymi. Because UEA-1 specifically recognizes mature mTECs, this finding is consistent with a severe defect in the maturation process of the medullary component. It is accepted that RANK ligand (RANKL), CD40 ligand (CD40L), and lymphotoxin (LT) in CD4 SP cells provide differentiating signals for mTEC and AIRE expression.[28] Despite the substantial CD40L, RANKL and

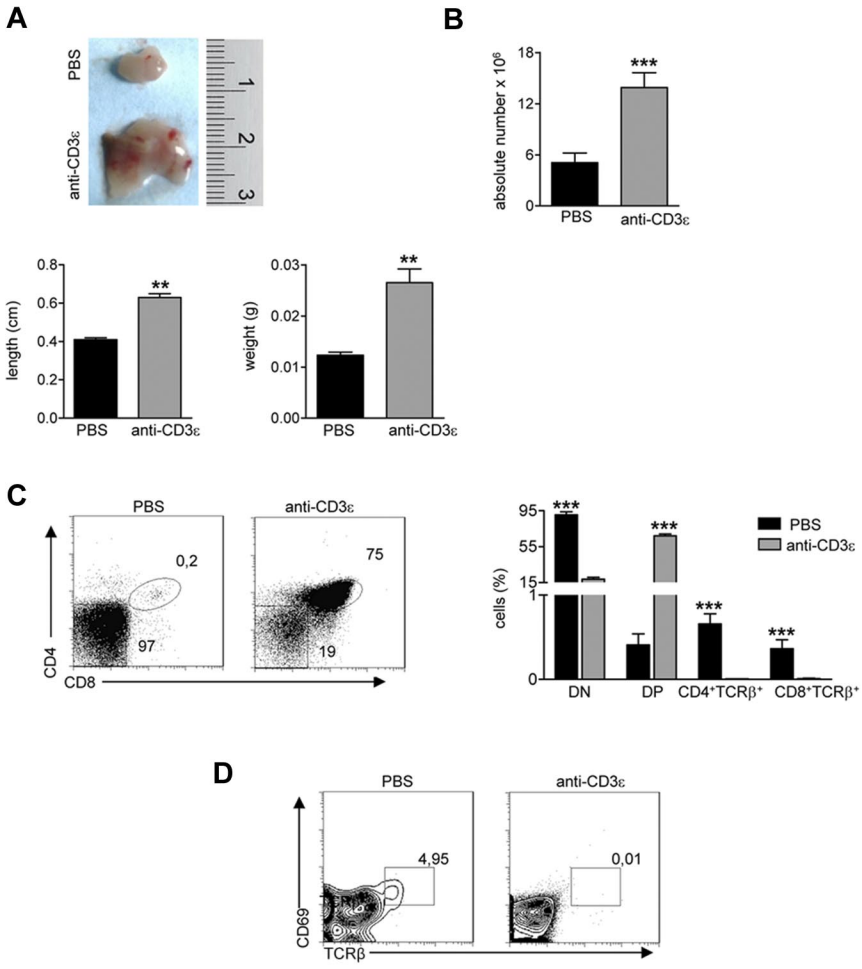

Figure 2. Anti-CD3ε mAb treatment induces *RAG2*^{R229Q} thymic expansion and DN to DP transition, without positive selection. *RAG2*^{R229Q} mice were intraperitoneally injected at the 3rd and 13th day after birth with 25 μg of anti-CD3ε mAb or PBS and killed 2 months after last injection. (A top) Macroscopic aspect of a representative *RAG2*^{R229Q} thymus from mice treated with PBS or anti-CD3ε mAb. (Bottom) Length and weight of thymi from the 2 groups (n = 5); $^{**}P = .0079$. (B) Absolute number of thymic cells from *RAG2*^{R229Q} mice injected with PBS (n = 17) and anti-CD3ε mAb (n = 20); $^{***}P < .0001$. (C left panel) Representative dot plots of thymocyte distribution from the indicated mice. (Right panel) Graph shows the frequency of DN, DP, CD4$^+$TCRb$^+$ SP, and CD8$^+$TCRβ$^+$ SP populations in PBS (n = 15) and anti-CD3ε mAb (n = 21) treated mice; $^{***}P < .0001$. (D) Representative dot plots of CD69 and TCRβ expression in DP population of indicated mice; the percentage of CD69$^+$TCRβ^{high} cells is represented.

LTα mRNA levels in *RAG2*^{R229Q} CD4 SP cells (data not shown), we did not detect any AIRE expression in *RAG2*^{R229Q} thymi (Figure 1D). We further defined the epithelial cell defect in *RAG2*^{R229Q} thymus by flow cytometry studies. Mutant mice showed an increased proportion of cTECs defined as CD45$^-$MHCII$^+$Ly51$^+$ (*RAG2*^{R229Q} 79.1 ± 5.7 vs RAG2$^{+/+}$ 37.6 ± 1.44), while immature mTECs (MHCII^{low}Ly51$^-$mTECs^{low}) and mature mTECs (MHCII^{high}Ly51$^-$, mTECs^{high}) were greatly reduced in comparison with age-matched control mice (mTECs^{low} 19.4 ± 5.14 vs 47.6 ± 1.7 and mTECs^{high} 0.7 ± 0.2 vs 12.3 ± 3.2; Figure 1E left). As expected, absolute counts obtained after enzymatic digestion of the entire thymi confirmed the severe depletion of these subsets (Figure 1E right). Accordingly, we observed a significant down-regulation of mRNAs encoding AIRE and several TRAs such as cytochrome P450 (CytP450), fatty acid–binding protein (FABP), Insulin2, and glutamic acid decarboxylase 67 (GAD67; Figure 1F). Overall, these results suggest that severely impaired mTEC differentiation in *RAG2*^{R229Q} thymi might lead to defective negative selection and escape of autoreactive T-cell clones to the periphery.

Anti-CD3ε mAb administration in *RAG2*^{R229Q} newborns improves maturation of thymic medulla

Injection of anti-CD3ε mAb into RAG2$^{-/-}$ mice promotes DN to DP stage transition[21,23] mimicking pre-TCR signal transduction[29] and inducing thymocyte/stroma cross-talk events generated by thymocyte β selection.[22] Ten days after intravenous injection of anti-CD3ε mAb, RAG2$^{-/-}$ thymi showed cortical-medullary compartmentalization[22] and significant improvement of the M/C (supplemental Figure 1A, available on the *Blood* Web site; see the Supplemental Materials link at the top of the online article). Moreover, thymi from treated mice showed a positive binding for UEA-1, whereas staining with AIRE-specific Abs was negative (supplemental Figure 1B). Based on these results, we investigated the effect of anti-CD3ε mAb administration in our mutant mice. To prevent stimulation of circulating mature T cells and consequent cytokine secretion,[30] we treated *RAG2*^{R229Q} newborns, which are devoid of mature T cells both in the thymus and in the spleen (supplemental Figure 2). We intraperitoneally injected 3-day-old *RAG2*^{R229Q} mice with 25 μg of anti-CD3ε mAb, and repeated the injection 10 days later. The mice were followed for 2 months and showed normal growth and no apparent side effects. On sacrifice, thymi from treated mice showed an expansion in size (Figure 2A top and bottom) and greater cellularity (Figure 2B). Moreover, an increase in the percentage of DP cells correlating with a decreased frequency of DN cells (Figure 2C) was evident in treated animals. Of note, SP thymocytes expressing TCRβ were dramatically reduced on treatment. Consistently, DP cells from treated mice lacked CD69$^+$ TCRβ$^+$ cells indicating lack of thymocyte-positive selection (Figure 2D). The improvement of thymic architecture in treated mice was indicated by the formation of medullary foci and the presence of distinct corticomedullary demarcation with a significant increase of the M/C (Figure 3A). Staining with CK5 and CK8 further corroborated this conclusion by revealing thymic compartmentalization of the 2 isoforms in anti-CD3ε mAb but not

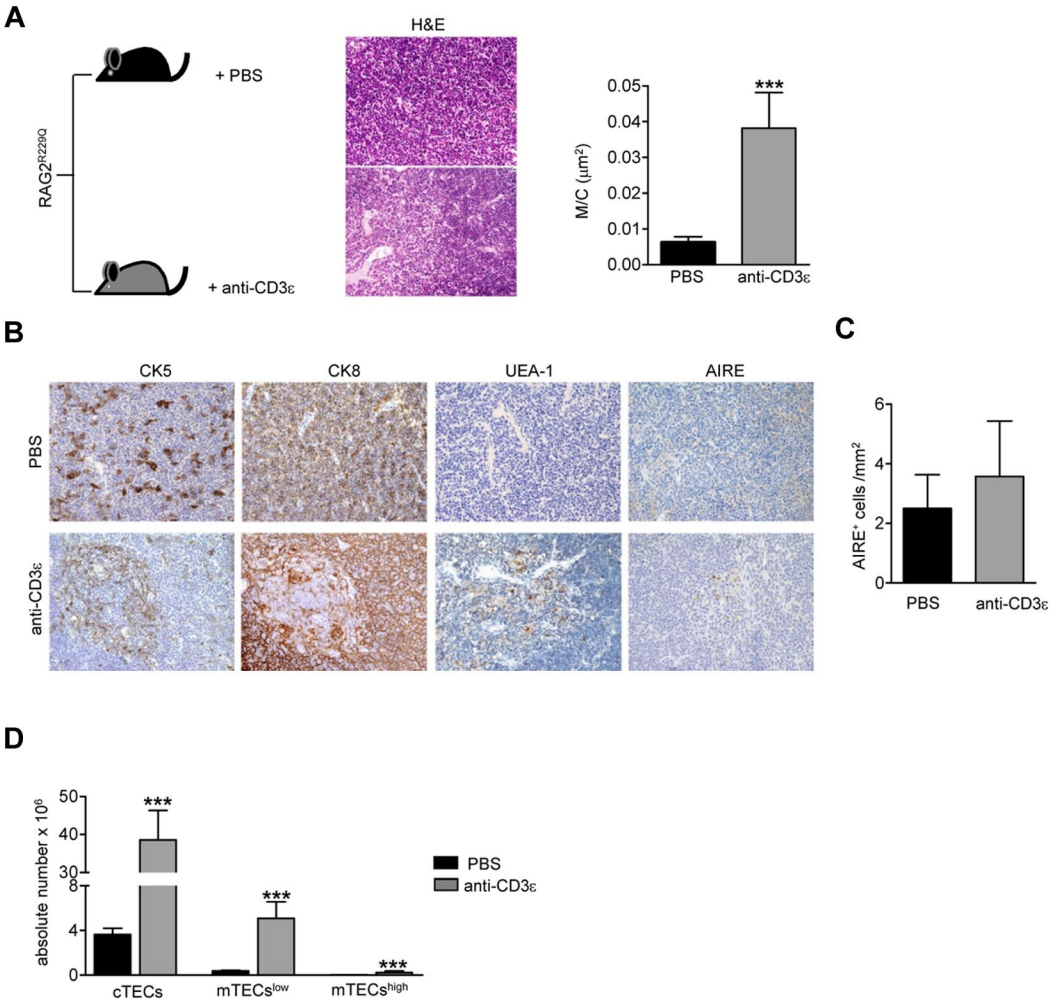

Figure 3. Improvement of thymic epithelium in *Rag2*^{R229Q} mice 2 months after anti-CD3ε mAb administration. (A) Representative H&E staining of a thymus obtained from PBS and anti-CD3ε mAb-treated *RAG2*^{R229Q} newborns (original magnification, ×20). (Right panel) Graphic representation of M/C ratio in the 2 groups (PBS n = 8, anti-CD3ε n = 9); ***P = .0003. (B) CK5, CK8, UEA-1, and AIRE immunohistochemistry of thymus from mice treated as indicated (original magnification, ×20). (C) Quantitative analysis of AIRE$^+$ cells obtained as described in "Analysis of the ratio between medullary and cortical area and tissue-infiltration score" in PBS (n = 6) and anti-CD3ε mAb (n = 10) mice. (D) Absolute number of different epithelial cell subsets obtained after enzymatic digestion of thymi from PBS and anti-CD3ε mAb mice (n = 5); **P = .0079.

saline-treated mice. Despite a slight increase in UEA-1 binding, UEA-1$^+$ cells did not form clusters as fully mature mTECs[25] expressing AIRE (Figure 3B) do. Accordingly, we detected very rare and slightly stained AIRE$^+$ cells as further confirmed by quantitative data obtained by careful immunohistochemical analysis (Figure 3C). This finding is consistent with the absence of SP cells in treated thymi; indeed, the same result was obtained in RAG2$^{-/-}$ mice (see previous paragraph). Of note, we found a significant increase in absolute counts of all thymic epithelial subsets, which confirmed the effect of anti-CD3ε mAb on the proliferation of thymic epithelium[22] (Figure 3D).

Anti-CD3ε mAb administration in adult *RAG2*^{R229Q} mice has poor effect on thymic epithelial development

To confirm that neonatal treatment is preferable to adult treatment to promote thymus development in *RAG2*^{R229Q} mice, we compared the M/C in adults and newborns 1 and 2 months after anti-CD3ε mAb injection. The increase in the M/C in the neonatal mice was significant at 1 month and remained so 2 months after injection, whereas we did not observe any substantial changes in the adult (Figure 4A). Histologic analysis of the *RAG2*^{R229Q} thymi of the mice treated in adult life showed a very slight change in the general architecture of the organ (revealed by H&E staining) although some changes in the distribution of CK5$^+$ and CK8$^+$ cells were present (Figure 4B). Moreover, UEA-1 and AIRE were not detectable (data not shown).

Anti-CD3ε mAb treatment in *RAG2*^{R229Q} newborns reduces peripheral T-cell activation and tissue infiltration

Anti-CD3ε mAb administration resulted in a dramatic reduction of peripheral CD4$^+$ and CD8$^+$ cells in lymph nodes (LNs; Figure 5A). We have previously shown that 80% to 90% of *RAG2*^{R229Q} CD4$^+$ and CD8$^+$ peripheral lymphocytes display an activated phenotype and once stimulated produce an excessive amount of Th1 cytokines.[13] Of note, a reduction in the percentage of effector/memory (EM) cells defined as CD44$^+$ CD62L$^-$ together with an increase of the naive (CD44$^-$ CD62L$^+$) compartment was clearly evident in the CD8$^+$ subset (Figure 5B) of anti-CD3 mAb-treated *RAG2*^{R229Q} mice. Despite a lack of significant reduction of CD4 with the EM phenotype, stimulation of T cells from anti-CD3ε mAb-treated mice with PMA and ionomycin revealed a significant reduction of both IFN-γ and TNF-α secreting cells (Figure 5C). To evaluate

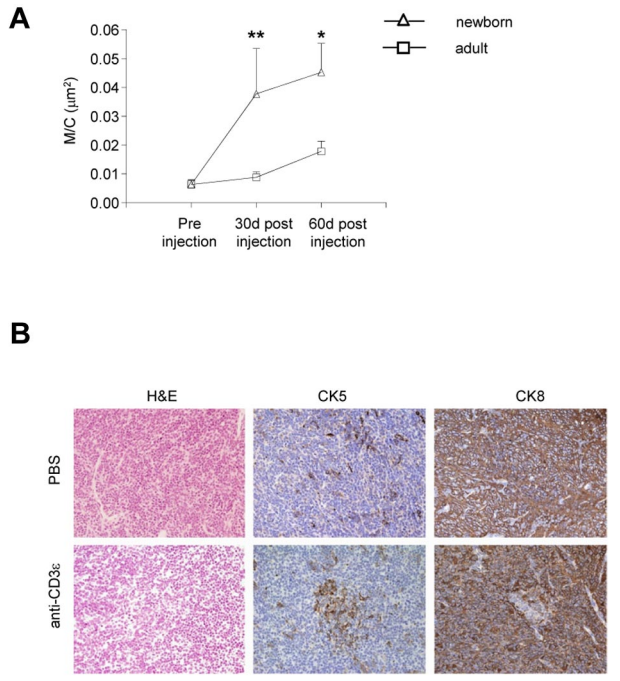

Figure 4. Poor effect of anti-CD3ε mAb administration on thymic epithelium in adult *RAG2*^{R229Q} mice. (A) Comparison between the M/C obtained in newborns and adults *RAG2*^{R229Q} mice 1 and 2 months after anti-CD3ε mAb treatment (statistical analysis was done between the 2 groups newborns versus adults); **P* = .0286, ***P* = .0041. (B) H&E, CK5 and CK8, immunohistochemistry of thymi from PBS, and anti-CD3ε mAb treated mice (original magnification, ×20).

whether treatment with anti-CD3ε mAb resulted in amelioration of tissue infiltration by T cells, we quantified CD4$^+$ and CD8$^+$ cells in the skin, gut, liver, and lung. A dramatic reduction in CD4$^+$ and CD8$^+$ infiltration index (Figure 5D) was observed in anti-CD3ε mAb-treated mice compared with the control group. This result correlated with reduced tissue damage in treated mice (Figure 5E). We did not find any significant difference in peripheral tissue infiltration grade in adult treated mice compared with controls, further corroborating the observation that anti-CD3ε mAb treatment in adults is not as efficient as in newborns (supplemental Figure 3).

Anti-CD3ε mAb treatment in *RAG2*^{R229Q} newborns results in reduction of serum Ig levels

We have previously described that the production of serum IgG1, IgG2, and IgM was preserved in *RAG2*^{R229Q} mice, whereas IgG3 and IgA were reduced. Consistent with the OS phenotype, IgE levels were significantly higher in mutant mice.[14] Indeed, *RAG2*^{R229Q} mice showed an enlarged compartment of immunoglobulin-secreting cells (ISC) in all lymphoid organs because of an exaggerated T-cell activation. To verify whether the anti-CD3ε mAb treatment could influence serum Ig production and in particular IgE levels, we measured the concentrations of Ig subtypes in the sera of treated mice and respective controls. A dramatic drop in Ig production was detected 2 months after the treatment, suggesting that the lack of T-cell help impaired class switch recombination. We also observed a significant decrease in IgM levels, which we ascribed to the amelioration of tissue damage with consequent reduction of circulating danger-associated molecular pattern (DAMP) molecules, which promote plasma cell generation[31] (Figure 6).

Anti-CD3ε–mediated thymus development positively affects the selection of *RAG2*^{R229Q} T-cell progenitors

Anti-CD3ε mAb treatment in *RAG2*^{R229Q} newborns resulted in peripheral lymphopenia presumably because of severely impaired T-cell development by premature termination of the recombination process at TCR loci and consequent lack of TCRβ-expressing thymocytes.[32] This renders it difficult to assess whether anti-CD3ε mAb-mediated thymus development might improve the selection of the emerging oligoclonal *RAG2*^{R229Q} TCR repertoire. Therefore, we treated RAG2$^{-/-}$ mice with a single intravenous injection of anti-CD3ε mAb or PBS as control. Ten days later, we transplanted sublethally irradiated mice with 10^6 *RAG2*^{R229Q} E13.5 fetal liver (FL) cells. Three months after transplantation, only mice treated with anti-CD3ε mAb showed persistent thymic expansion with signs of maturation, such as typical lobulation and foci of cortical-medullary demarcation as well as CK5 and CK8 compartmentalization. Moreover, the M/C was significantly increased confirming the expansion of the medulla (Figure 7A). In addition, we observed the appearance of UEA-1$^+$ and AIRE$^+$ cells in treated mice (Figure 7B). Quantitative analysis by detailed immunohistochemical analysis (see "Histology"), confirmed the significant induction of AIRE expression by anti-CD3ε mAb treatment in combination with adoptive transfer of *RAG2*^{R229Q} hematopoietic progenitors (Figure 7C). Analysis of T cells from treated chimeric mice showed a significant reduction in the proportion of EM cells in both CD4$^+$ and CD8$^+$ subsets together with a concomitant increase of the naive compartment (Figure 7D). In striking contrast to the group of untreated chimeric mice, which developed alopecia and skin erythroderma similarly to *RAG2*^{R229Q} mice, the animals receiving anti-CD3ε mAb did not show any skin alteration. Consistently, histologic analysis of tissue sections obtained from various organs (skin, lung, liver and gut) revealed a dramatic reduction of tissue infiltrating cells in treated mice (Figure 7E).

All together these data demonstrate that development of *RAG2*^{R229Q} thymocytes in an "anti-CD3ε primed" recombinase-deficient thymic environment dramatically ameliorates the pathogenic potential of the resulting peripheral T cell pool, suggesting that early treatment with anti-CD3ε mAb might be beneficial in SCID patients with poor thymus.

Discussion

Patients with OS and leaky SCID show a severe defect in thymic epithelial maturation and AIRE expression[15,16] and an analogous picture is present in the *RAG2*^{R229Q} mouse, which faithfully recapitulates human OS.[13] Indeed, further characterization of *RAG2*^{R229Q} thymus in the present study revealed lack of mTECs^{high} and reduced expression of AIRE and TRAs. To investigate whether the altered thymus microenvironment might play a role in the pathogenesis of autoimmunity in OS, we exploited the potential effect of anti-CD3ε mAb treatment to mimic pre-TCR signaling in immature thymocytes and induce the thymocyte/epithelial cross-talk required for medullary epithelium differentiation. To avoid toxicity associated with massive cytokine release from mature T cells on anti-CD3ε mAb administration[30] we treated *RAG2*^{R229Q} mice early in life when only few peripheral T cells are present. Two months after the treatment, thymus analysis showed a significant amelioration of the M/C, a notable improvement of the distribution of CK5 and CK8, and more importantly, the onset of mTECs binding UEA-1, a marker of medullary differentiation. It has been reported that positively selected thymocytes are responsible for

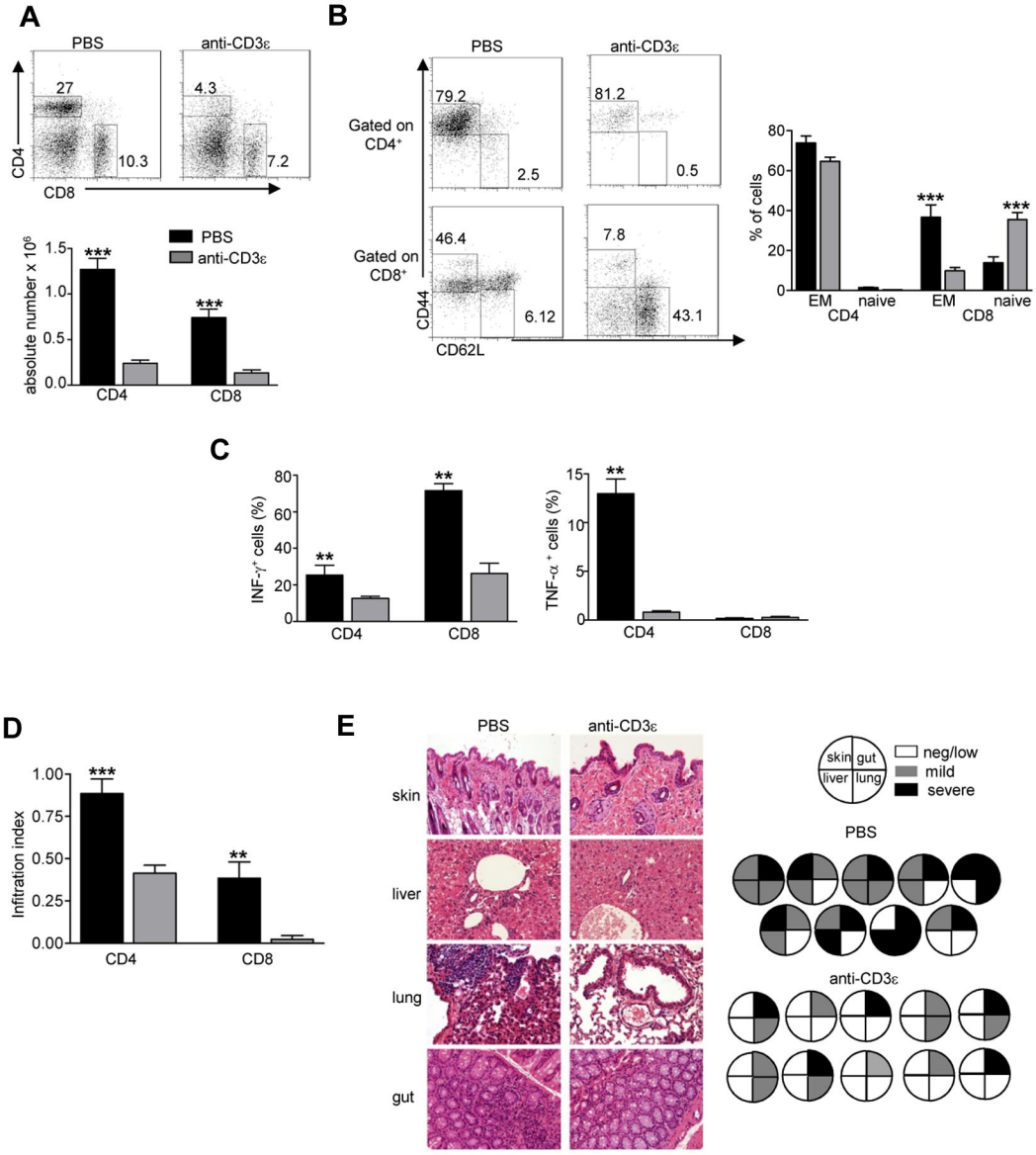

Figure 5. Anti-CD3ε mAb administration in *RAG2*^{R229Q} newborns reduces activation of peripheral T cells and prevents immunopathology. (A top), Representative dot plots of CD4$^+$ and CD8$^+$ populations in LNs of PBS and anti-CD3ε mAb-treated *RAG2*^{R229Q} mice; numbers represent the percentages of cells within the indicated regions. (Bottom) Absolute numbers of CD4$^+$ and CD8$^+$ cells in LNs of PBS (n = 12) and anti-CD3ε mAb (n = 21) *RAG2*^{R229Q} mice; ***$P < .0001$. (B left), Representative dot plots with the distribution of naive and EM cells within CD4$^+$ and CD8$^+$ LNs cells in PBS and anti-CD3ε mAb *RAG2*^{R229Q} mice. (Right) Statistics of the percentage of EM and naive cells in CD4$^+$ and CD8$^+$ subsets from PBS (n = 13) and anti-CD3ε mAb-treated mice (n = 21). (C) Graphic representation of the percentage of CD4$^+$ and CD8$^+$ cells producing the indicated cytokines obtained by intracellular staining in LNs from PBS and anti-CD3ε mAb *RAG2*^{R229Q} mice (n = 5); **$P = .0079$. (D) Infiltration index of CD4$^+$ and CD8$^+$ cells (see "Analysis of the ratio between medullary and cortical area and tissue-infiltration score") in several organs (liver, lung, skin, and gut) of mice treated with PBS (n = 10) and anti-CD3ε mAb (n = 11); ***$P = .0006$, **$P = .0034$. (E left) Representative H&E staining of skin, lung, liver, and gut from PBS and anti-CD3ε–treated mice (original magnification, ×20). (Right) Pie charts show global infiltration grade in each organ calculated from H&E staining as described in "Analysis of the ratio between medullary and cortical area and tissue-infiltration score." Each pie represents a mouse from 1 of the 2 groups.

complete mTEC maturation[28,33]; indeed, in our model very few AIRE$^+$ cells were observed in accordance with the poor SP-cell generation. Nevertheless, in contrast with saline-treated animals, in which peripheral CD8$^+$ cells displayed an EM phenotype, peripheral CD8$^+$ cells from newborns treated with anti-CD3ε mAb displayed a naive phenotype, suggesting that they might have been selected in a tolerogenic thymic environment. We did not observe a significant reduction of CD4$^+$ cells with EM phenotype in treated mice, which might be because of homeostatic expansion of few positively selected thymocytes in the peripheral lymphopenic environment of *RAG2*^{R229Q} mouse. However, staining for proinflammatory cytokines revealed a dramatic reduction of IFN-γ and TNF-α secreting CD4$^+$ cells. Analysis of peripheral tissue infiltration demonstrated a significant decrease of organ infiltrates in target tissues such as skin, liver, lung, and gut, thereby demonstrating that anti-CD3ε mAb treatment has a beneficial impact on *RAG2*^{R229Q} mice immunopathology. Consistently, serum IgE levels, which have been widely described as important in the pathogenesis of OS,[14,34] were barely detectable in anti-CD3ε mAb-treated mice. The treatment proved to be effective and did not provoke any clinical signs of autoimmunity or tissue infiltration or other adverse effects in mice followed up to 5 months (data not shown). Abs targeting CD3 molecules are potent immunosuppressive agents and have been extensively used in patients undergoing transplantation to avoid rejection.[35-37] Furthermore, short-term administration of anti-CD3ε–specific Ab in NOD mice has been shown to induce

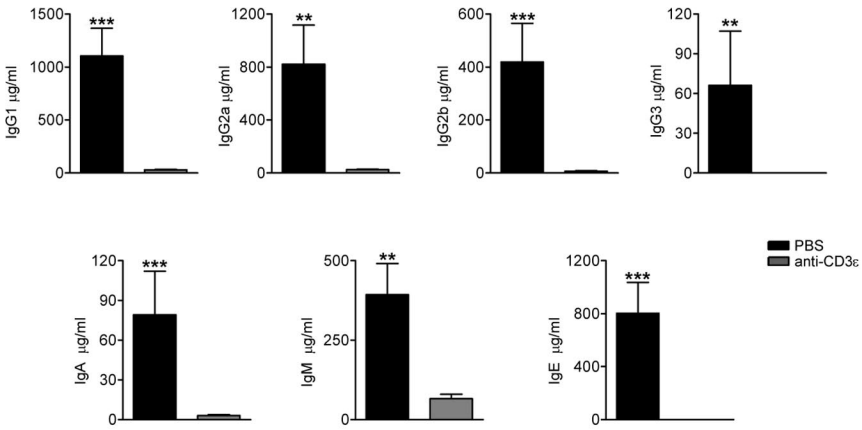

Figure 6. Anti-CD3ε mAb treatment in *RAG2*^{R229Q} newborns decreases serum Ig levels. Sera from PBS (n = 11) and anti-CD3ε mAb (n = 8) mice were collected and run in duplicate to obtain the concentration of the different Ig subsets; ***P = .0003, **P = .0041.

long-term remission of type I diabetes.[38] In addition to their capacity to alter immunoresponse via TCR modulation, anti-CD3 Abs might exhibit mitogenic properties and induce cytokine release with deleterious consequences for patients.[39] Nonmitogenic Ab variants have been generated to avoid such adverse events and have been used in different murine models of disease or clinical trials[40-43] although their efficacy is still a matter of debate.[44] On the other hand, side effects of mitogenic anti-CD3ε mAb can be minimized with a low-dose therapy.[36,45] The beneficial effect of anti-CD3ε mAb treatment we observed in *RAG2*^{R229Q} mice is likely because of an improved thymic selection process. It remains to be determined whether the effect of anti-CD3ε mAb on thymus architecture can be achieved with only "mitogenic Abs" because until now the impact of nonmitogenic Abs on thymus development has not been addressed. To further understand whether anti-CD3ε mAb-mediated thymus development might per se prevent the pathologic effect of hypomorphic *RAG2*^{R229Q} T cells, we transplanted a high number of *RAG2*^{R229Q} hematopoietic progenitors into RAG2$^{-/-}$ mice, previously injected with anti-CD3ε mAb to induce medullary expansion. Three months after the transplantation, no sign of tissue infiltrations has been observed in those mice receiving the Ab; conversely, devastating erythroderma and organ damage were present in the cohort of control mice. Remarkably, at odds with the treated *RAG2*^{R229Q} newborns, these chimeras showed AIRE expression in the thymic medulla and a significant decrease of EM cells in both the CD4$^+$ and CD8$^+$ subset. The appearance of AIRE$^+$ mTECs in this model might derive from the increased T-cell development in this experimental setting compared with injected *RAG2*^{R229Q} newborns, in which inhibition of Vβ gene rearrangement by anti-CD3ε mAb dramatically affects T-cell maturation beyond the DP stage.[32] Therefore, anti-CD3ε mAb thymus conditioning without affecting T-cell developmental potential of pre-T cells further improved OS phenotype. Overall, these findings demonstrate that, despite the T-cell autonomous *RAG* defect, thymic stromal induction can avoid the differentiation of pathogenic T cells infiltrating peripheral tissues. Based on these results, we propose the early administration of anti-CD3ε Abs as an adjuvant therapy for OS or SCID patients with poorly developed thymus while waiting for available bone marrow donors. Because OS patients, differently from SCID cases, can present variable numbers of peripheral autoreactive T cells, a careful dosage of the compound would be required to avoid a massive release of cytokines as reported in individuals undergoing organ transplantation.[46] Once an efficacious and safe dose for SCID infants has been determined, we assume that, besides preventing organ infiltration, the anti-CD3ε mAb treatment could boost thymic reconstitution in candidate SCID patients for cellular therapies. Overall, the present study provides the first evidence that, beyond the elimination of autoreactive T cells, anti-CD3ε mAb treatment directly acts on thymic structure and prevents the onset of immunopathology by generating an appropriate thymic environment for selection of a tolerant T-cell repertoire. Finally, this treatment could be also considered in the future, once safe lentiviral vectors are available, to improve the efficacy of gene therapy of leaky forms of V(D)J recombination characterized by autoimmunity and poorly developed thymus.

Acknowledgments

The technical assistance of Enrica Mira Catò and Tanja Rezzonico is acknowledged.

This work was supported by the European Commission's 7th Framework Programs: 261387-CELL-PID, Fondazione Telethon (TGT11A03) to A.V. and Fondazione Cariplo (A.V., P.L.P., and F.G.). The research was partially supported by Minister of Health RF2009-1485896. F.F. was supported by a Marie Curie International Reintegration Grant.

Authorship

Contribution: V. Marrella designed and performed research, analyzed data, and wrote the manuscript; P.L.P., E.F., and M.C. performed histologic analyses; A.C., V. Maina, B.C., F.S., and M.P. contributed to performing experiments; F.F and E.T. analyzed data; P.V. contributed to the revision of the manuscript; and F.G. and A.V. designed the research, analyzed data, and wrote the manuscript.

Conflict-of-interest disclosure: The authors declare no competing financial interests.

Correspondence: Anna Villa, Milan Unit, Istituto di Ricerca Genetica e Biomedica, Consiglio Nazionale delle Ricerche, Via Fantoli 16/15, 20138 Milan, Italy; e-mail: anna.villa@humanitasresearch.it; or Fabio Grassi, Institute for Research in Biomedicine, Via Vincenzo Vela 6–CH-6500 Bellinzona, Switzerland; e-mail: fabio.grassi@irb.unisi.ch.

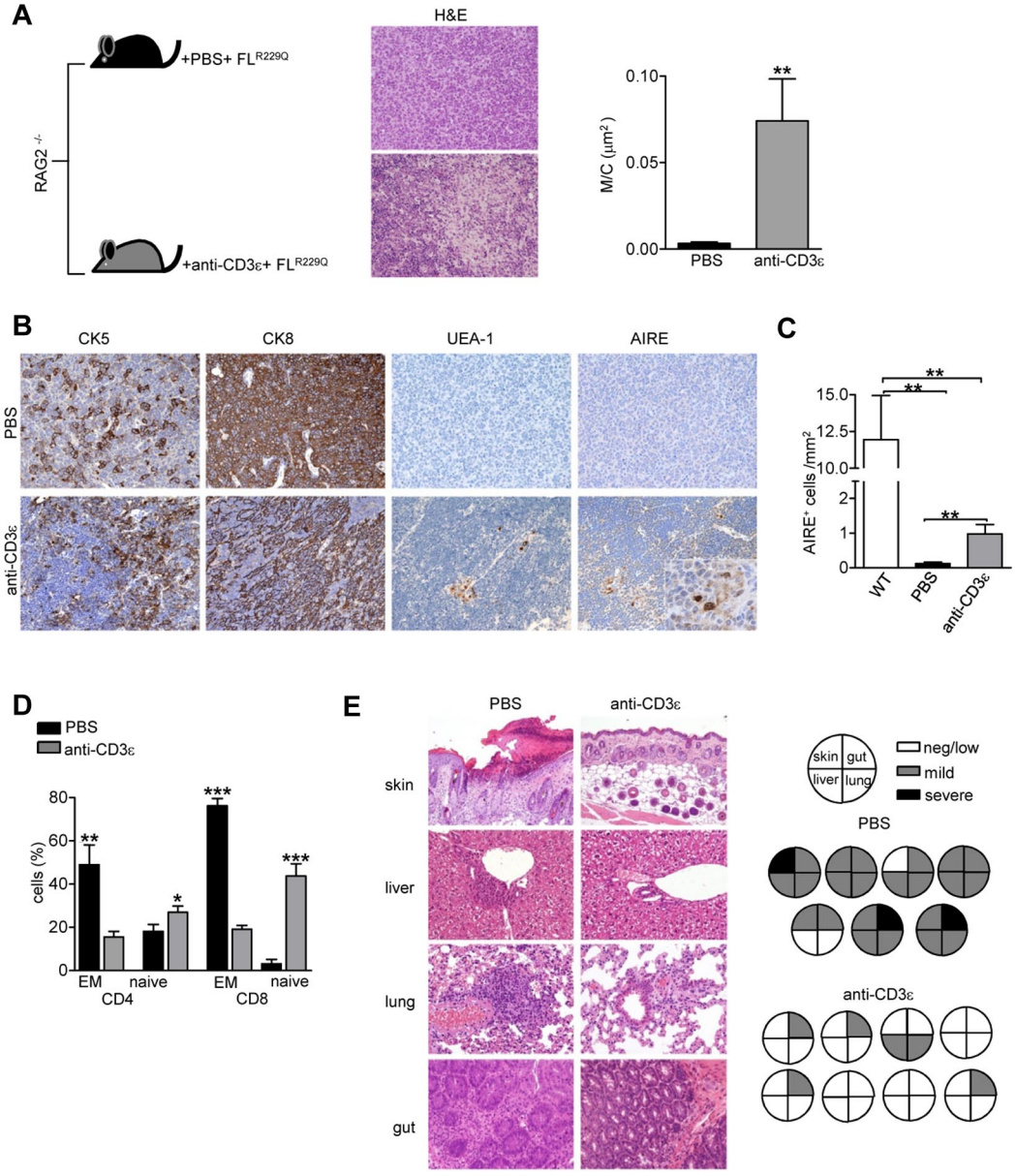

Figure 7. Anti-CD3ε mAb-mediated thymus development positively affects the selection of *Rag2*^{R229Q} T-cell progenitors (indicated as FL^{R229Q}). (A) Representative H&E staining of a thymus from PBS and anti-CD3ε mAb-treated chimeric mice (original magnification, ×20) and graphic representation of the M/C in the 2 groups (PBS n = 6, anti-CD3ε mAb n = 8); $^{**}P = .008$. (B) Immunohistochemistry of thymi from PBS and anti-CD3ε mAb-treated mice (original magnification, ×20). In AIRE panel, the inset shows magnification of AIRE$^+$ cells induced by the treatment (original magnification, ×40). (C) Quantitative analysis of thymic AIRE$^+$ cells obtained as described in "Methods" in wild-type mice, chimeric mice treated with PBS (n = 6) and chimeric mice treated with anti-CD3ε mAb (n = 8); $^{**}P = .007$ (D) Percentages of EM and naive cells within the donor-derived CD4$^+$ and CD8$^+$ populations in the 2 groups (n = 7); $^{**}P = .0028$, $^{***}P < .0001$. (E left) H&E staining of skin (original magnification, ×10), lung, liver, and gut (original magnification, ×20) from PBS and anti-CD3ε mAb chimeric mice. (Right) Pie charts show global infiltration grade in each organ calculated from H&E staining as described in "Histology." Each pie indicates tissue infiltration in individual mouse in the 2 groups.

References

1. Omenn GS. Familial reticuloendotheliosis with eosinophilia. *N Engl J Med.* 1965;273:427-432.
2. Villa A, Santagata S, Bozzi F, et al. Partial V(D)J recombination activity leads to Omenn syndrome. *Cell.* 1998;93(5):885-896.
3. Villa A, Santagata S, Bozzi F, Imberti L, Notarangelo LD. Omenn syndrome: a disorder of Rag1 and Rag2 genes. *J Clin Immunol.* 1999; 19(2):87-97.
4. Brugnoni D, Airo P, Facchetti F, et al. In vitro cell death of activated lymphocytes in Omenn's syndrome. *Eur J Immunol.* 1997;27(11):2765-2773.
5. de Saint-Basile G, Le Deist F, de Villartay JP, et al. Restricted heterogeneity of T lymphocytes in combined immunodeficiency with hypereosinophilia (Omenn's syndrome). *J Clin Invest.* 1991; 87(4):1352-1359.
6. Rieux-Laucat F, Bahadoran P, Brousse N, et al. Highly restricted human T cell repertoire in peripheral blood and tissue-infiltrating lymphocytes in Omenn's syndrome. *J Clin Invest.* 1998;102(2): 312-321.
7. Signorini S, Imberti L, Pirovano S, et al. Intrathymic restriction and peripheral expansion of the T-cell repertoire in Omenn syndrome. *Blood.* 1999;94(10):3468-3478.
8. Cavazzana-Calvo M, Andre-Schmutz I, Dal Cortivo L, Neven B, Hacein-Bey-Abina S, Fischer A. Immune reconstitution after haematopoietic stem cell transplantation: obstacles and anticipated progress. *Curr Opin Immunol.* 2009; 21(5):544-548.
9. Gozdzik J. Rapid full engraftment and successful immune reconstitution after allogeneic hamatopoietic stem cell transplantation with reduced intensity conditioning in Omenn syndrome. *Pediatr Transplant.* 2009;13(6):760-765.
10. Mazzolari E, Moshous D, Forino C, et al. Hematopoietic stem cell transplantation in Omenn syndrome: a single-center experience. *Bone Marrow Transplant.* 2005;36(2):107-114.
11. Corneo B, Moshous D, Gungor T, et al. Identical

mutations in RAG1 or RAG2 genes leading to defective V(D)J recombinase activity can cause either T-B-severe combined immune deficiency or Omenn syndrome. *Blood.* 2001;97(9):2772-2776.

12. Villa A, Sobacchi C, Notarangelo LD, et al. V(D)J recombination defects in lymphocytes due to RAG mutations: severe immunodeficiency with a spectrum of clinical presentations. *Blood.* 2001; 97(1):81-88.
13. Marrella V, Poliani PL, Casati A, et al. A hypomorphic R229Q Rag2 mouse mutant recapitulates human Omenn syndrome. *J Clin Invest.* 2007; 117(5):1260-1269.
14. Cassani B, Poliani PL, Marrella V, et al. Homeostatic expansion of autoreactive immunoglobulin-secreting cells in the Rag2 mouse model of Omenn syndrome. *J Exp Med.* 2010;207(7): 1525-1540.
15. Cavadini P, Vermi W, Facchetti F, et al. AIRE deficiency in thymus of 2 patients with Omenn syndrome. *J Clin Invest.* 2005;115(3):728-732.
16. Poliani PL, Facchetti F, Ravanini M, et al. Early defects in human T-cell development severely affect distribution and maturation of thymic stromal cells: possible implications for the pathophysiology of Omenn syndrome. *Blood.* 2009; 114(1):105-108.
17. Anderson M. Aire and T cell development. *Curr Opin immunol.* 2011;23(2):198-206.
18. Kyewski B, Klein L. A central role for central tolerance. *Annu Rev Immunol.* 2006;24:571-606.
19. Honig M, Schwarz K. Omenn syndrome: a lack of tolerance on the background of deficient lymphocyte development and maturation. *Curr Opin Rheumatol.* 2006;18(4):383-388.
20. Notarangelo LD, Gambineri E, Badolato R. Immunodeficiencies with autoimmune consequences. *Adv Immunol.* 2006;89:321-370.
21. Jacobs H, Vandeputte D, Tolkamp L, de Vries E, Borst J, Berns A. CD3 components at the surface of pro-T cells can mediate pre-T cell development in vivo. *Eur J Immunol.* 1994;24(4):934-939.
22. Porcellini S, Panigada M, Grassi F. Molecular and cellular aspects of induced thymus development in recombinase-deficient mice. *Eur J Immunol.* 1999;29(8):2476-2483.
23. Shinkai Y, Alt FW. CD3 epsilon-mediated signals rescue the development of CD4+CD8+ thymocytes in RAG-2−/− mice in the absence of TCR beta chain expression. *Int Immunol.* 1994;6(7): 995-1001.
24. Leo O, Foo M, Sachs DH, Samelson LE, Bluestone JA. Identification of a monoclonal antibody specific for a murine T3 polypeptide. *Proc Natl Acad Sci U S A.* 1987;84(5):1374-1378.
25. Poliani PL, Vermi W, Facchetti F. Thymus microenvironment in human primary immunodeficiency diseases. *Curr Opin Allergy Clin Immunol.* 2009;9(6):489-495.
26. Anderson G, Jenkinson EJ, Rodewald HR. A roadmap for thymic epithelial cell development. *Eur J Immunol.* 2009;39(7):1694-1699.
27. Takahama Y. Journey through the thymus: stromal guides for T-cell development and selection. *Nat Rev Immunol.* 2006;6(2):127-135.
28. Hikosaka Y, Nitta T, Ohigashi I, et al. The cytokine RANKL produced by positively selected thymocytes fosters medullary thymic epithelial cells that express autoimmune regulator. *Immunity.* 2008; 29(3):438-450.
29. Grassi F, Barbier E, Porcellini S, von Boehmer H, Cazenave PA. Surface expression and functional competence of CD3-independent TCR zeta-chains in immature thymocytes. *J Immunol.* 1999; 162(5):2589-2596.
30. Ferran C, Sheehan K, Dy M, et al. Cytokine-related syndrome following injection of anti-CD3 monoclonal antibody: further evidence for transient in vivo T cell activation. *Eur J Immunol.* 1990;20(3):509-515.
31. Marichal T, Ohata K, Bedoret D, et al. DNA released from dying host cells mediates aluminum adjuvant activity. *Nat Med.* 2011;17(8):996-1002.
32. Mathieu N, Spicuglia S, Gorbatch S, et al. Assessing the role of the T cell receptor beta gene enhancer in regulating coding joint formation during V(D)J recombination. *J Biol Chem.* 2003; 278(20):18101-18109.
33. Naspetti M, Aurrand-Lions M, DeKoning J, et al. Thymocytes and RelB-dependent medullary epithelial cells provide growth-promoting and organization signals, respectively, to thymic medullary stromal cells. *Eur J Immunol.* 1997;27(6):1392-1397.
34. Ozcan E, Notarangelo LD, Geha RS. Primary immune deficiencies with aberrant IgE production. *J Allergy Clin Immunol.* 2008;122(6):1054-1062; quiz 1063-1054.
35. Cosimi AB, Colvin RB, Burton RC, et al. Use of monoclonal antibodies to T-cell subsets for immunologic monitoring and treatment in recipients of renal allografts. *N Engl J Med.* 1981;305(6):308-314.
36. Flechner SM, Goldfarb DA, Fairchild R, et al. A randomized prospective trial of low-dose OKT3 induction therapy to prevent rejection and minimize side effects in recipients of kidney transplants. *Transplantation.* 2000;69(11):2374-2381.
37. A randomized clinical trial of OKT3 monoclonal antibody for acute rejection of cadaveric renal transplants. Ortho Multicenter Transplant Study Group. *N Engl J Med.* 1985;313(6):337-342.
38. Chatenoud L, Thervet E, Primo J, Bach JF. Anti-CD3 antibody induces long-term remission of overt autoimmunity in nonobese diabetic mice. *Proc Natl Acad Sci U S A.* 1994;91(1):123-127.
39. Chatenoud L. Anti-CD3 antibodies: towards clinical antigen-specific immunomodulation. *Curr Opin Pharmacol.* 2004;4(4):403-407.
40. Herold KC, Gitelman S, Greenbaum C, et al. Treatment of patients with new onset type 1 diabetes with a single course of anti-CD3 mAb teplizumab preserves insulin production for up to 5 years. *Clin Immunol.* 2009;132(2):166-173.
41. Utset TO, Auger JA, Peace D, et al. Modified anti-CD3 therapy in psoriatic arthritis: a phase I/II clinical trial. *J Rheumatol.* 2002;29(9):1907-1913.
42. Steffens S, Burger F, Pelli G, et al. Short-term treatment with anti-CD3 antibody reduces the development and progression of atherosclerosis in mice. *Circulation.* 2006;114(18):1977-1984.
43. Bluestone JA, Auchincloss H, Nepom GT, Rotrosen D, St Clair EW, Turka LA. The Immune Tolerance Network at 10 years: tolerance research at the bedside. *Nat Rev Immunol.* 2010; 10(11):797-803.
44. You S, Chatenoud L. New generation CD3 monoclonal antibodies: are we ready to have them back in clinical transplantation? *Curr Opin Organ Transplant.* 2010;15(6):720-724.
45. Chatenoud L. Immune therapy for type 1 diabetes mellitus-what is unique about anti-CD3 antibodies? *Nat Rev Endocrinol.* 2010;6(3):149-157.
46. Chatenoud L. Progress towards the clinical use of CD3 monoclonal antibodies in the treatment of autoimmunity. *Curr Opin Organ Transplant.* 2009; 14(4):351-356.